Final Draft

of the original manuscript

Kandelhard, F.; Georgopanos, P.:

Predici as a Polymer Engineers' Tool for the Synthesis of Polymers via Anionic Polymerization.

In: Industrial & Engineering Chemistry Research. Vol. 60 (2021) 30, 11373 - 11384.

First published online by American Chemical Society: 16.07.2021

https://dx.doi.org/10.1021/acs.iecr.1c01319

Predici as a polymer engineers' tool for the synthesis of polymers via anionic polymerization

Felix Kandelhard and Prokopios Georgopanos*

Helmholtz-Zentrum Hereon, Institute of Membrane Research, Max-Planck-Str. 1, Geesthacht, 21502 Germany

E-mail: *prokopios.georgopanos@hereon.de

Phone: +49(0) 4152 87-2420. Fax: +49(0) 4152 87-2499

Abstract

In this study, the potential of a combined reaction kinetics model and a heat transfer model for the process development and scale-up of polystyrene synthesis via anionic polymerization, which is later extended to a copolymerization with isoprene, is presented. In an innovative way, the program Predici was utilized to describe the requirements needed in the modeling of polymerization in larger scale. This model combines the precise description of the polymerization reaction kinetics and the prediction of macromolecular properties offered by the program Predici with a heat transfer model to predict safety-relevant parameters such as the temperature and pressure profiles of the reaction system. In this way, it enables the precise investigation of interactions between process parameters and product properties as well as opens the path to optimal process control. Furthermore, changes associated with the scale-up of the process were studied using the model. The developed model was successfully applied to all these tasks and could be used for fast screening in the development of polymer synthesis.

Introduction

Modeling and simulation are important tools in chemical process development that have gradually gained more importance over the last decades.[1,2] They can assist the development of processes in different areas ranging from product properties to heat and mass transfer behavior, which is influenced by the reactor type and geometry. One of these areas is the kinetics of the chemical reactions, which determines the reaction rates, product selectivity. In some cases, e.g., polymer synthesis, it even has impact on the physical properties of the products.[3] If the reaction is an exothermic, the kinetic are directly linked to the rate of heat generation, which is one of the most important safety-relevant parameters.[4] As all important polymerizations are exothermic reactions,[5] they are often accompanied by a strong increase of the reaction temperature. This phenomenon is known for many polymerization systems, especially in case of polymerization of vinyl monomers such as acrylates,[6] dienes or styrene.[7] The strong temperature increases can result in thermal runaway situations, making the heat generation rate a crucial safety parameter for polymerization processes.[7]

Many different programs and tools are used for modeling and simulation in research and industry. This includes specialized solutions developed in programming languages such as Fortran, C++, or Python, open-source applications, e.g., OpenFoam®[8,9] as well as commercial software like COMSOL Multiphysics®,[10] Aspen®, or Ansys®.[4,11,12] One of these commercial simulation tools is the program Predici, which was developed by M. Wulkow and was first introduced in the early nineties of the 20$^{\text{th}}$ century for the modeling of polymerization kinetics.[13] It uses the discrete Galerkin method to calculate the molar weight distributions of polymers[14] and was extended by a hybrid Monte Carlo approach[15] as well as functions for parameter estimation and optimization of process parameters.[16] The program Predici was successfully used in the past to model polymerization reactions ranging from free-radical polymerization performed in bulk,[17–20] solution,[21] suspension,[22] or emulsion;[23,24] controlled-radical polymerizations;[25–27] living anionic;[28,29] and step-growth polymerizations.[30,31] Anionic polymerizations were investigated by further model-based studies

for various reactor types and monomers.[32–38]

The focus of Predici lies on the modeling of the material balance with the associated chemical reaction kinetics but also offers the possibility to integrate heat balances.[16] In a recent study, the anionic polymerization of isoprene in cyclohexane carried out in laboratory and industrial scale was modeled with a different approach.[39] It is stated that Predici does not satisfy the requirements to model an industrial scale polymerization process, especially in the estimation of the thermal behavior of the reactor and its intrinsic risk potential. However, Predici offers the possibility to be customized by user scripts. An approach to model the thermal behavior of a chemical process in Predici is presented in this work. This is achieved by implementing an extended heat balance that includes the reaction volume as well as the reactor jacket. The heat balance parameters such as the heat transfer coefficients are estimated based on geometrical and material parameters using empirical correlations and dimensionless numbers. By using this approach, the model should enable a quick screening of the investigated reaction with regard to the heat transport behavior of the reactor system but still using the efficiency of Predici in the description of polymer reactions as well as theprediction of the polymer physical properties (e.g., molecular mass distribution).

Model

The model was developed using the program Predici Version11.Bayes3 (Dr. Michael Wulkow Computing in Technology GmbH, Rastede, Germany). Due to its focus on the modeling of polymerization kinetics, the program Predici contains many built-in functions that are helpful in the implementation of polymerization kinetics. Nevertheless, Predici also offers an open interface with its own scripting language that can be used to work on further model development (e.g., heat-balances, particle size distributions, or radial concentration gradients). These have to be representable in the form of algebraic and differential equations. Predici uses the assumption of an ideal mixed reactor. As the model system, the basic

system of an anionic polymerization of styrene conducted in cyclohexane (solvent) was chosen because the focus of this work lies in the implementation of the heat transfer model into Predici. In a second step, the model was extended in order to describe the copolymerization with isoprene for the synthesis of block or statistical copolymers. All simulations were carried out using the full distribution mode of Predici.[16]

The heat balance of a chemical process is influenced by the convective heat flow inside and outside of the reactor as well as other source terms, the most important one being the reaction heat. Because there is no convective mass and heat transfer entering or leaving the reactor in a batch process, the heat balance-equation could be simplified (see **Equation** 1). The amount of thermal energy accumulated in the reactor ($\dot{Q}_{Accumulation}$) is determined by the reaction heat ($\dot{Q}_{Reaction}$), the conductive heat transfer through the wall ($\dot{Q}_{Conductive}$), the frictional heat introduced by the stirrer ($\dot{Q}_{Stirrer}$), and additional heat sources ($\dot{Q}_{other}$) such as internal heaters. This approach was first utilized in the modeling of an evaporative-cooled process observed via reflux calorimetry.[40] The thermal energy is accumulated in the heat capacity of the reaction mixture as well as the reactor's material. The relative contribution of the reactor will decrease with increasing reactor size but is still an important factor within the orders of magnitude considered in this work. The masses and heat capacities of the reactor (stirrer plus wall) estimated for the calculations are summarized in the supporting information (**Table** S3).

$$\dot{Q}_{Accumulation} = \dot{Q}_{Reaction} + \dot{Q}_{Conduction} + \dot{Q}_{Stirrer} + \dot{Q}_{other} \tag{1}$$

The reaction heat is given by the product of the reaction rate (r), the volume of the reaction mixture (V_R), and the reaction enthalpy (ΔH_R). In a batch process, the reaction heat can only be directly influenced by the concentration of the reactants loaded into the reactor as well as the process temperature, which is mostly regulated via a heating or cooling jacket. For this reason, the conductive heat transfer from the tempering jacket through the reactor

wall with a surface area A_R is a crucial factor for the thermal safety of a chemical process. Therefore, it should closely be examined in process development. The heat flow is driven by the temperature gradient between the reactor (T_R) and the jacket (T_j) and is given by **Equation** 2.

$$\dot{Q}_{Conduction} = k \cdot A_R \cdot (T_R - T_j) \tag{2}$$

In this context, the thermal transmittance or overall heat transfer coefficient (k), which describes the heat transfer from the tempering jacket through the reactor wall into the reaction medium, is the central engineering parameter. The thermal transmittance can be divided into three separate heat transfer steps and calculated using the **Equation** 3. The first step is the heat transfer from the reaction medium to the reactor wall represented by the inner heat transfer coefficient (α_R). It is followed by the conductive heat transfer through the reactor wall characterized by the quotient of the thickness of the wall (d_{wall}) and the thermal conductivity of its material (λ_{wall}). The third step is the heat transfer from the reactor wall to the cooling/heating fluid of the jacket (α_j).

$$\frac{1}{k} = \frac{1}{\alpha_R} + \frac{d_{wall}}{\lambda_{wall}} + \frac{1}{\alpha_j} \tag{3}$$

The heat transfer coefficients can be derived from the dimensionless Nusselt-number ($Nu = \frac{\alpha \cdot L}{\lambda}$) for a specific characteristic length (L). Several empiric relationships exist, describing the dependency of the Nusselt-number from the flow conditions represented by the Reynolds-number ($Re = \frac{\rho \cdot v \cdot L}{\eta}$) and the thermal properties of the medium (Prandtl-number: $Pr = \frac{\eta \cdot c_p}{\lambda}$). Besides the flow velocity (v), physical properties that are important in this context are the density (ρ), the dynamic viscosity (η), the thermal conductivity (λ), and the specific heat capacity (c_p) of the fluids involved in the process. The applied Nusselt correlations, which are summarized in the supporting information (**Equation** S1-S6), are dependent on the stirrer type and taken from literature.[41] The jacket fluid used in

the simulations is modeled after the thermo-fluid Malotherm® XC. All physical parameters used in the equations are summarized in the supporting information (**Equation** S18-S21) and taken from the product data-sheet.[42] In the simulations, glass reactors with varying sizes between 0.5 L and 15.0 L are used. The geometrical data of the reactors are based on those of the Polyclave (0.5 L, 1.0 L, 2.0 L, and 5.0 L) and Kiloclave (15.0 L) series from Büchi (Büchi AG, Uster, Switzerland) and summarized in the supporting information (**Table** S1). The heat balance was implemented in Predici in the form of interconnected user scripts (see blue and red boxes in **Figure** 1) and is influenced by several parameters (orange boxes). The heat introduced by the stirrer is negligible and thus can be estimated using the Newton number (Ne, see **Equation** S43-S44).[43] This was done for different simulation results and shown in the supporting information (see **Figure** S2). The equations for these calculations are taken from literature.[44] The heat introduced by the stirrer during the reaction is well below 10% compared to the heat of reaction in all setups investigated. The reason for this is the highly diluted reaction solution, which leads to a less significant increase in viscosity.

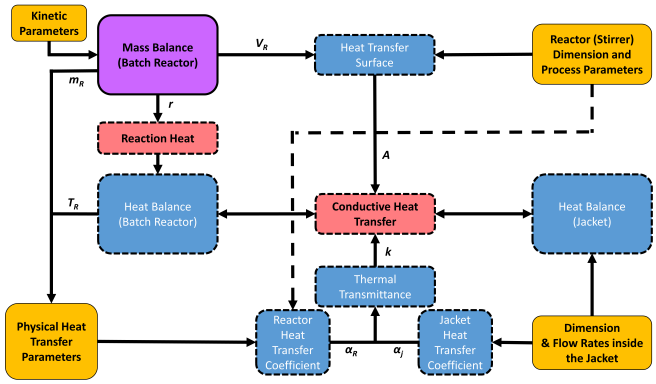

Figure 1: Schematic model structure showing the input parameter (orange), mass balance space (violet), and implemented scripts (dotted frame). The scripts are divided into heat balance scripts (red) and supporting scripts (blue). The arrows indicate how the variables and parameters are used in and transferred between the scripts.

The implemented heat-balance with an automated calculation of the heat transfer parameters makes it possible to quickly check the effect of parameter adjustments (e.g., polymerization recipe or temperature) on the thermal behavior of the chemical process. These data can assist in the scale-up of a polymerization process. To generate reliable and useful

data, it is necessary to have an exact knowledge of the reaction kinetics. If the kinetics of the reaction or crucial physical properties such as the viscosity of the reaction mixture, are not known from practice or literature, the model has to be carefully validated using experimental data.

This approach was tested based on the anionic polymerization of styrene conducted in cyclohexane. These reactions are often carried out in a temperature range of 30 °C to 60 °C. The polymerization kinetics are implemented in form of a model containing only the initiation, chain propagation, and deactivation steps (**Equation** 4 - 6). The involved species are the initiator *sec*-butyllithium ($s\text{-}BuLi$), the monomer styrene (St), the propagating polymer chain with n monomeric units ($P^*_{n,s}$), and the terminated polymer chain (P^{dead}_{m+n}). The rate coefficient of the initiation is calculated from the reaction rates reported by Hsieh.[45] The deactivation reaction step and its rate coefficient (k_d) describe a thermally driven LiH elimination that occurs at higher temperatures.[46,47] The propagation rate coefficient[48] (**Table** 1), as well as the physical properties of the involved species[4,39,44,49–51](see **Equation** S22-S37 in the supporting information), are taken from the literature. The viscosity of the polymer solution is calculated using a combination of the Mark-Houwink (**Equation** S39) and Huggins-equation(**Equation** S38 in the supporting information).[7,52] A similar approach was applied by Cortese et al. in a computational fluid dynamic study dealing with the anionic polymerization of styrene in micro reactors.[53] It should be noted that the viscosity model neglects the effect introduced by the aggregation of living chains. The heat of polymerization (ΔH_p) of styrene was set to -60 kJ mol^{-1}.[54]

$$s\text{-}BuLi + St \xrightarrow{k_i} P^*_{1,s} \tag{4}$$

$$P^*_{n,s} + St \xrightarrow{k_{p,ss}} P^*_{n+1,s} \tag{5}$$

$$P^*_n \xrightarrow{k_d} P^{dead}_n \tag{6}$$

Table 1: Reaction rate coefficients of the initiation (k_i), propagation ($k_{p,ss}$), and deactivation step (k_d) for the anionic polymerization of styrene carried out in cyclohexane with *sec*-BuLi as the initiator. The constants are written in form of temperature-dependent Arrhenius parameters with the frequency factor (A_f) and the activation energy divided by the universal gas constants ($\frac{E_a}{R}$). The rate coefficient of the initiation is calculated from the reaction rates reported by Hsieh.[45]

Rate Coefficient	A_f [different units]	$\frac{E_a}{R}$ [K]
k_i	$8.85 \cdot 10^9 [\mathrm{s}^{-1}]$	$7.18 \cdot 10^3$
$k_{p,ss}$[48]	$7.73 \cdot 10^9 [\mathrm{L}^{0.5}\,\mathrm{mol}^{-0.5}\,\mathrm{s}^{-1}]$	$8.25 \cdot 10^3$
k_d[47]	$3.92 \cdot 10^6 [\mathrm{s}^{-1}]$	$8.70 \cdot 10^3$

The anionic species involved in the polymerization form different aggregates depending on their properties and their interaction with the solvent. In case of the initiator *sec*-BuLi, there are different findings in the literature concerning this behavior and its effects on the reaction order.[55] While the reaction order of *sec*-BuLi in aromatic solvents is four, some studies reported a reaction order of nearly one in the case of aliphatic solvents such as cyclohexane.[45,55] Living polystyrene anions with their counter-ion lithium arrange themselves as dimers in cyclohexane.[48,56] Due to this aggregates, the reaction order concerning the living chain is also changed. This effect could be represented in the model using effective rate coefficients for the initiation and propagation reactions that are functions of the initiator and chain concentrations. Because different reaction orders for *sec*-BuLi are given in literature, a first-order reaction was assumed for the model. The effective rate coefficient of the propagation reaction can be calculated using **Equation** 7 based on the finding of Steube *et. al.*.[48] The equation is slightly adapted in order to fit into Predici's framework. As there are no chains formed at the beginning of the simulated reaction, the propagation rate coefficients are instead dependent on the initiator concentration in the first simulation step to prevent a division by zero error in the computation.

$$\frac{d[M]}{dt} = -k_{p,ss} \cdot [P^*_{n,s}]^{\frac{1}{2}} \cdot [M] = -\underbrace{\frac{k_{p,ss}}{[P^*_{n,s}]^{\frac{1}{2}}}}_{k_{p,ss,eff}} \cdot [P^*_{n,s}] \cdot [M] \tag{7}$$

In a second step, the kinetic model is extended to a copolymerization model that includes isoprene as the second monomer. This extended model adds the propagation step of isoprene as well as cross polymerization steps between living chains with either of the two monomers. The extended copolymerization model is described in more detail in the supporting information (**Equation** S7-S17). The rate coefficients and copolymerization parameters,[48] as well as the temperature-dependent functions of the physical parameters of isoprene, are taken from the literature.[39,57]

In addition to the heat transfer behavior, the pressure inside the reactor is another important safety parameter. The pressure in the reactor (p_R) is calculated from the partial pressure of the components (p_i) in the reaction mixture, their mole fraction (x_i, which can be derived from the concentration values of the species), and the pressure of the non-condensable material ($\bar{p}_0$) using an equation (**Equation** 8) already applied in a recent study.[39] All values of pressure are given in the unit bar. The calculation of the pressure of the non-condensable material is shown in the supporting information (**Equation** S40).

$$p_R = \bar{p}_0 + \sum_i x_i \cdot p_i \tag{8}$$

The temperature-dependent partial pressure is determined with the Antoine-equation (**Equation** 9). The Antoine equation parameters for styrene, isoprene, and cyclohexane are summarized in **Table** S4 in the supporting information.[58–60]

$$ln(p_i) = A - \frac{B}{C + T} \tag{9}$$

Results

As already mentioned, the above described process model used combines the simulation of safety-relevant parameters centered around the thermal behavior of the reactor with the strength of Predici in the prediction of polymer properties. To show the capability of this model, the anionic polymerization of styrene in cyclohexane was investigated regarding the influence of parameters in three areas. First, the reaction mixture and conditions in form of the monomer content and starting temperature. Second, the effects of different process parameters regarding the stirrer and jacket of the reactor, and third the changes in the reactor scale (scale-up). In a last step the extended copolymerization model was tested. The performance of the model is evaluated using four simulated process variables, the monomer conversion (from now on referred to as conversion), the number average molar mass of the polymer (referring to the polymer molecular characteristics), the temperature of the reaction mixture, and the pressure inside the reactor. This work focuses exclusively on the development and implementation of the model and its predictions with regard to the questions mentioned above. However, it is important to carefully validate the model based on experimental data in future studies. The reaction calorimetry is a method which could be used to validate heat transfer parameters such as the heat transfer coefficients as well as the reaction heat. The heat transfer coefficients are calculated by the model using empirical correlations, which assumes ideal conditions as for example an ideal flow behavior in the jacket, and are known to have varying degrees of deviation from the experiments.[41,43] Furthermore, some material properties, especially the viscosity have to be experimentally validated.

Temperature and Monomer Content

Initially, the starting temperature was varied between 20 °C and 60 °C with a monomer content of 5, 10, 20, and 30 wt% with a target molecular weight of 100 kg mol^{-1}. All reactions are simulated in a 0.5 L stirred tank reactor with a spiral stirrer (diameter: 40 mm), and a stirring speed of 250 min^{-1}. The inlet-temperature of the thermo-fluid was set to the starting temperature with a volume flow rate of 10 L min^{-1}. The simulated temperature and conversion profiles are shown in **Figure** 2. Due to the strong differences in the reaction rates introduced by concentration and temperature, the profiles for are plotted with a logarithmic scale for better visualization.

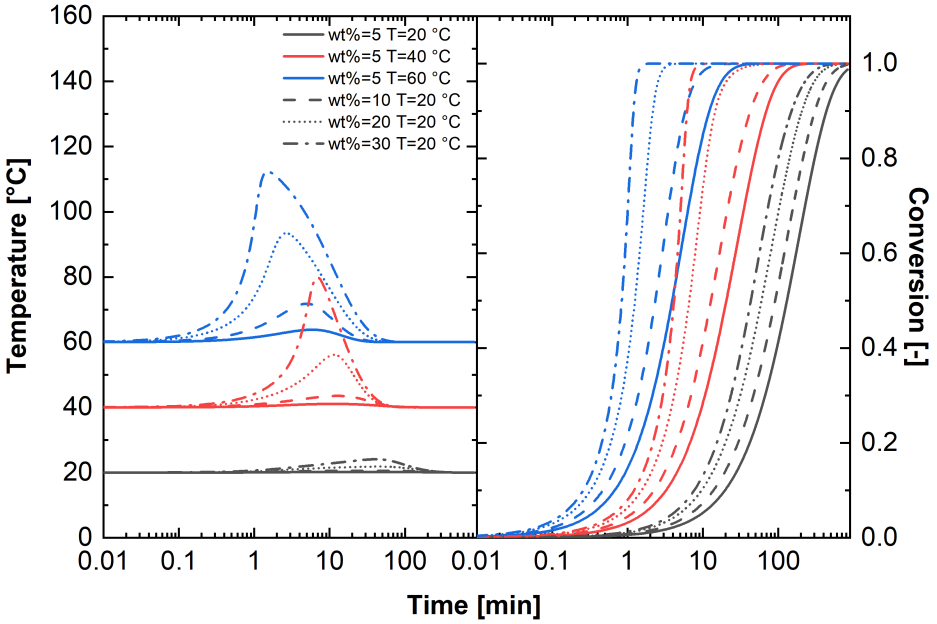

Figure 2: Simulated temperature and conversion profiles for varying monomer content (5 wt%: straight lines, 10 wt%: dashed lines, 20 wt% dotted lines, and 30 wt%: dashed/dotted lines) and starting temperature (20 °C: black, 40 °C: red, and 60 °C: blue)

As it can be seen in the conversion profiles, the anionic polymerization of styrene in cyclohexane is very sensitive to the change of temperature and the monomer concentration. The faster reaction rates are accompanied by an equally fast rise in the temperature due to the high reaction heat which is released in a shorter time frame. To quantify this effect, a couple of parameters were extracted from the simulated data. In **Table** 2, the time after

conversion of 0.95 was reached ($t_{0.95}$), the number average molecular mass at this conversion ($\overline{M}_{n,0.95}$), the maximal temperature (T_{max}), and the time in which it was reached (t_{max}) as well as the maximal pressure (p_{max}) are summarized. Although anionic polymerizations can reach nearly full conversion, a value of 0.95 conversion was selected to measure the reaction time. This facilitates the comparability of the different simulations because the reactions become very slow at the end.

Table 2: Simulated time with 0.95 conversions ($t_{0.95}$), the number average molecular mass ($\overline{M}_{n,0.95}$) at this point, maximal reaction temperature (T_{max}), and time in which this temperature is reached (t_{max}) as well as maximal pressure (p_{max}) for varying monomer content and starting temperature.

Polymer Content [%]	T_S [°C]	$t_{0.95}$ [min]	$\overline{M}_{n,0.95}$ [kg mol^{-1}]	T_{max}[°C]	t_{max} [min]	p_{max} [bar]
5	20	569	95.2	20.2	14	1.10
	40	91	93.3	41.1	11	1.32
	60	16	92.4	63.8	6	1.70
10	20	402	95.1	20.6	37	1.10
	40	58	92.8	43.5	13	1.34
	60	7	92.0	71.8	5	1.85
20	20	273	92.1	21.8	44	1.11
	40	19	92.4	56.1	11	1.47
	60	2	92.3	93.4	3	2.35
30	20	205	94.3	41.0	24	1.17
	40	7	92.0	80.0	7	1.81
	60	1	92.3	112.4	2	2.92

The reaction time in which a conversion of 0.95 is reached drops from 569 min (20 °C and 5 wt%) to approximately 1 min (60 °C and 30 wt%). The maximum temperature is also reached earlier (after 2 min) and is higher (112 °C) for the highest monomer content and starting temperature. The reaction temperature increases by over 52 °C, which is only 20 °C lower than the adiabatic temperature rise (see supporting information **Equation** S41) of 70 °C at these reaction conditions. This occurs due to the fact that the heat dissipation through the cooling jacket with a maximum of 65 W is far slower than the heat flow generated by the reaction with a maximum of 914 W. The pressure rises much higher (up to 2.92 bar) compared to the other tested reaction set-ups. It has to be noted that anionic polymerization in praxis is rarely performed with a monomer content higher than 20 wt%. However, the

strength of a modeling approach is the ability to go to regions that are not feasible in reality. A further increase of the monomer content to 50 wt% would lead to a maximum temperature of over 180 °C, a pressure of over 4.8 bar and an increase in viscosity to over 14 Pa s. Such strong changes in temperature should be avoided in order to assure a safe reaction control. The reactions carried out at 60 °C with either 10 wt% or 20 wt% are also accompanied by a temperature increase of 12 °C and 33 °C as well as a maximum pressure of 1.85 bar and 2.35 bar. Depending on the recipe and temperature, the viscosity rises from 0.1 mPa · s up to 3.2 Pa · s for the highest monomer content of 30 wt%. The simulated viscosity profiles are summarized in the supporting information (**Figure** S1).

One of the most dangerous scenarios that can occur in exothermic chemical processes is a thermal runaway situation. In this case, the temperature increased by the reaction heat leads to a self acceleration of the reaction rate. Thermal runaways have been the cause of many major accidents in the history of the chemical industry, such as the Seveso disaster of 1976.[61] Because of the danger associated with thermal runaways, many criteria to prevent such an incident have been developed by engineers and scientists. A work of Van Welsenaere and Froment has shown that the difference between the temperature of the reaction mixture and the coolant temperature should not exceed the term of $\frac{R \cdot T_R^2}{E_a}$.[61,62] The simulated reactions were evaluated according to this criterion (**Table** 3).

All reactions simulated with a monomer content above 20 wt% and a temperature above 40 °C do not meet the criterion. Therefore, these formulations have the risk of leading to a thermal runaway of the process. The reactions with 5 wt% and 10 wt% can be carried out safely. This corresponds to the results of the study by Rodriguez-Guadarrama, who found that the polymerization of isoprene could be carried out safely up to a monomer content of 20 wt%.[39]

Table 3: Evaluation of the runaway risk of reactions carried out with varying temperatures and monomer content. A comparison of the maximum temperature difference between reactor and jacket temperature ($\Delta T_{R-J,max}$) as well as the term ($\frac{R \cdot T_R^2}{E_a}$) is given. Whether this criterion is fulfilled by the reaction is indicated by the check marks and crosses.

Polymer Content [%]	T_S [°C]	$\Delta T_{R-J,max}$ [K]	$\frac{R \cdot T_R^2}{E_a}$ [K]	Did criterion meet?
5	20	0.2	10.7	✓
	40	1.1	12.3	✓
	60	3.8	14.1	✓
10	20	0.6	10.7	✓
	40	3.5	12.4	✓
	60	11.8	14.8	✓
20	20	1.8	10.8	✓
	40	16.1	13.5	×
	60	33.4	16.7	×
30	20	21.0	12.2	×
	40	40.0	15.5	×
	60	52.4	18.4	×

Another method to further evaluate the risk associated with a process is the reaction trajectory plotted in the temperature/conversion plane. As the conversion is a dimensionless quantity, the temperature is also converted to a dimensionless temperature θ to be able to better compare different trajectories. The dimensionless temperature (θ) is calculated (Equation 10) from the activation energy of the propagation step (E_a), the universal gas constant (R), the jacket temperature (T_j), and the temperature of the reaction mixture (T_R).

$$\theta = \frac{E_a}{R \cdot T_j} \frac{T_R - T_j}{T_j} \tag{10}$$

In the adiabatic case, θ increases linearly with the conversion. The adiabatic trajectory can be calculated from the integration of an equation developed by Balakotaiah et al. and can be used as a benchmark for the simulated or experimental data.[61,63] This procedure is exemplarily shown in **Figure** 3 for the reactions carried out at 60 °C.

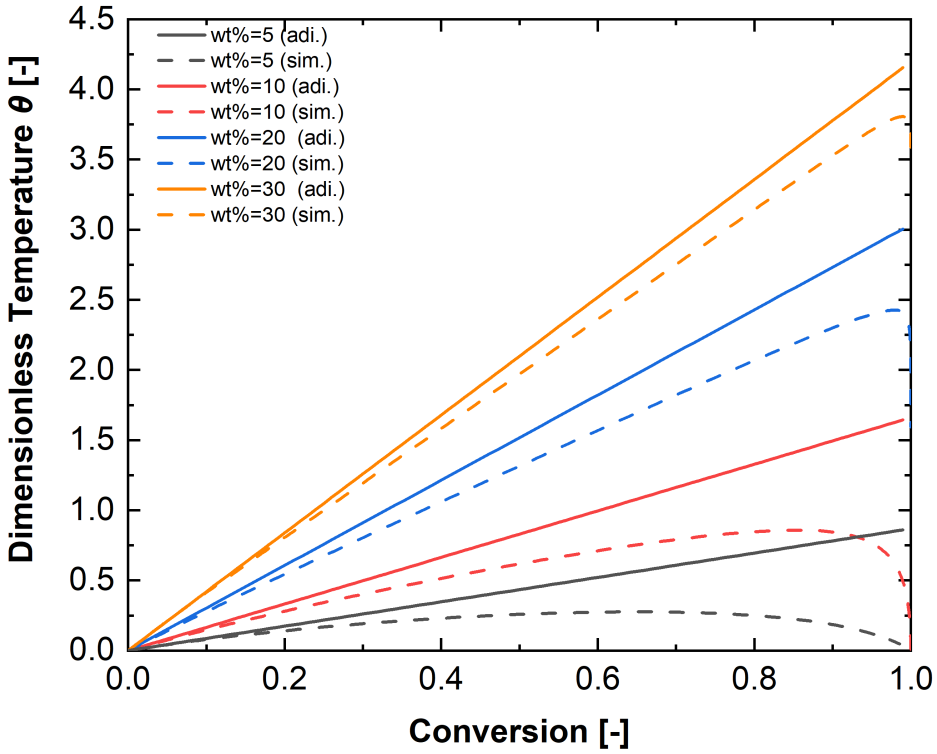

Figure 3: Dimensionless temperature trajectories plotted against the conversion for four reactions carried out at 60 °C with varying monomer content (between 5 wt% and 30 wt%). The straight lines represent the theoretical adiabatic case and the dashed lines are the simulated trajectories.

The trajectories in the temperature as a function of conversionconversion plane also show that the risk of a thermal runaway is significantly higher for reactions carried out with 20 wt% and 30 wt% compared to the ones with lower monomer content. Especially in the case of a reaction with 30 wt%, the trajectory nearly follows the theoretical adiabatic case. Balakotaiah et. al. have defined (based on findings of Adler and Enig) that if the second derivative of the reaction trajectory stays negative (negative curvature), the process will be insensitive to a runaway behavior.[63,64] The reaction carried out with 30 wt% even shows positive values in the second derivative at some conversions.

Both evaluations concerning the risk of runaway behavior confirm that reactions with more than 10 wt% carried out with the proposed reactor set-up and process parameters are not safe to handle and carry the risk of leading to a thermal runaway. This corresponds to the results of the study by Rodriguez-Guadarrama, who found that the polymerization

of isoprene could be carried out safely up to a monomer content of 20 wt%.[39] The reaction with 10 wt% carried out at 60 °C is also only slightly below the safety criteria and should be further optimized regarding the thermal behavior. It should be also kept in mind that these criteria were developed to investigate experimentally obtained data. The kinetic model used in this study does not include possible secondary and side reactions that could occur at a higher temperature and further accelerate the heat generation rate in the process. In the case of styrene, one of these side reactions could be the thermal self-initiation via a Diels-Alder reaction, which could start a radical process in addition to the planned anionic polymerization.[7,65] Therefore, the process settings that are considered safe by this simulation should be further evaluated by experimental methods in particular calorimetric measurements. It should also be noted that in industrial applications most anionic polymerization of vinyl monomers are carried out in thermal runaway conditions as it is shown by Rodriguez-Guadarrama for butadiene-styrene block copolymerisation.[66] This is only possible by a careful selection of process parameters in order to assure that these reaction still remain in a controllable process window concerning the temperature and pressure.

The reaction process could be adjusted with a couple of measures to come closer to an isothermal process. One way would be to change the process from a batch to a semi-batch process. This approach is often used to control highly exothermic and fast reactions and was applied for the anionic polymerization of styrene carried out in tetrahydrofuran on an industrial scale in a study of Saban et al.[37] However, the semi-batch reaction is not the focus of this work. The increase in temperature could also be influenced by different process parameters coupled to the stirring of the reaction mixture.

Heat Transfer Parameters

The reaction with 10 wt% monomer content carried out at 60 °C was chosen to investigate the heat transfer parameters. The influence of the volume flow rate of the thermo-fluid in the reactor jacket (varied between 5 L min^{-1} and 10 L min^{-1}), the temperature of the thermo-fluid (varied between 40 °C and 60 °C), the stirrer speed (varied between 150 min^{-1} and 350 min^{-1}), and the stirrer type on the heat transfer behavior were examined.The stirrer types included a Paravisc and an anchor-stirrer, both with a diameter of 68 mm, an inclined blade stirrer with four blades and a diameter of 40 mm, and a standard spiral stirrer (40 mm). All parameters were varied independently while the other three were kept constant according to the standard settings (i.e., the same settings used in the first simulations). The simulated data sets were evaluated with regard to their temperature profiles (**Figure** 4).

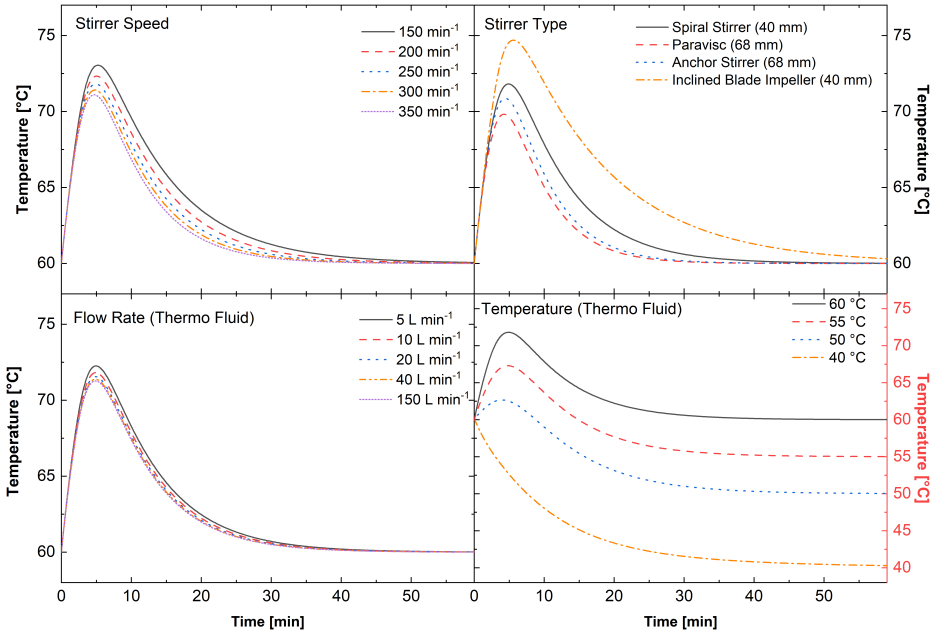

Figure 4: Simulated temperature profiles of reactions with varied heat transfer parameters. The investigated parameters are the stirrer speed (upper left), stirrer type (upper right), the volume flow rate of the thermo-fluid (lower left), and the temperature of the thermo-fluid (lower right).

The investigated parameters show a varying degree of influence on the temperature behavior of the reactor. The temperature of the thermo-fluid has the strongest effect because it directly influences the driving force of each heat transfer process, because it directly influences the temperature gradient, which is driving force of every heat transfer process. There is also an additional indirect effect on the thermal transmittance of the reactor wall. Lowering the jacket temperature by 10 °C reduces the temperature increase induced by the reaction heat to only about 2.67 °C (compared to 11.8 °C with standard settings). A gradient of 20 °C totally changes the form of the temperature profile with no observation of a maximum in the temperature profile. However, this could influence the conversion of the reaction or the product properties. These values in form of the time after conversion of 0.95 are reached ($t_{0.95}$, given in decimal minutes) and the number average mass at this point ($\overline{M}_{n,0.95}$) are summarized in **Table** S5. It also contains the maximum temperature (T_{max}) reached.

The effect of the changed jacket temperature on the conversion behavior is clearly visible in the time after 0.95 conversion is reached. The reaction time increases from 7.5 min to 40.4 min when the jacket temperature is lowered from 60 °C to 40 °C. At the same time, the $\overline{M}_{n,0.95}$ is nearly staying on the same level. Therefore, it is possible to produce a product with similar properties but in a longer reaction.

The flow rate in the jacket, the stirring speed as well as the stirrer type have an indirect influence on the heat transfer by affecting the thermal transmittance (k). Compared to the changes introduced by the jacket temperature, their effects on the maximal temperature are much smaller but also vary from one another. The type of the stirrer has the strongest influence. Specifically, using an inclined blade stirrer leads to a maximum reaction temperature of 74.70 °C, while the Paravisc could remove the heat in the most efficient way, reducing the maximal temperature to 69.83 °C. This behavior could be expected because the stirrer type changes the flow field inside the reactor, which determines the material transport and the convective proportion of the heat flow coupled to it. While the impact on the material transport, which could also strongly influence the reaction by introducing concentration or

temperature gradients inside the reactor, is not captured by the model, the direct effect on the convective heat transfer from the reaction solution on the reactor wall (inner heat transfer coefficient) is included in the computation of the Nusselt number. The introduction of gradients inside the reactor is a very interesting and important topic that was already investigated by some studies experimentally as well as based on modeling. (e.g., computational fluid dynamics).[4,11,12,61] However, this is not part of this work due to the assumption of an ideally mixed reactor.

The effect of the volume flow rate and stirring speed on the maximum temperature lies in the range of 2-3 °C. It could be observed that their impact becomes weaker with increasing flow rates or stirring speeds. This behavior could also be observed in the thermal transmittance (**Figure** 5).

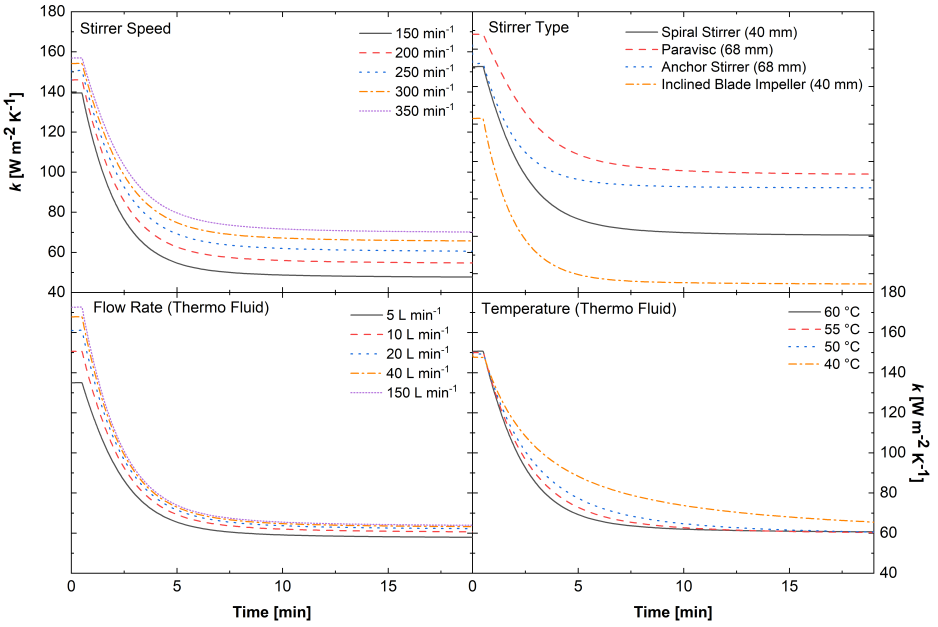

Figure 5: Change in the simulated thermal transmittance over the course of the reaction for varied volume flow rates of the thermo-fluid, stirring speed, and stirrer type.

At the beginning of the reaction, the thermal transmittance values are in the region between 120 W m^{-2} K^{-1} and 160 W m^{-2} K^{-1} depending on the setting of the heat transfer parameters. These values of the thermal transmittance correspond to data known from literature for batch reactors.[67] After the polymerization is started, the thermal transmittance decreases with increasing conversion due to the change of the viscosity.

The simulation results show that the model is able of accurately describing changes in the heat transfer behavior of polymerizations introduced by the variation of different parameters. This could be used to study the consequences associated with a scale-up of the polymerization as described in the following paragraph.

Scale-Up

The scale-up of the polymer synthesis process comes with some major challenges. Nevertheless, it is important in order to enable the utilization of polymer materials for a variety of applications such as fabrication of membranes, nonporous structures, or other materials. The simulation results shown so far were based on a small-scale polymerization reaction. However, due to the necessity for the production of larger polymer amounts, the scale-up of the synthesis of homo- and copolymers is investigated via modeling and simulation as well.

First, the surface-to-volume ratio of the reactor will decrease, resulting in lower cooling capacity because the rate of heat generation scales with the volume, while the heat removal happens through the reactor surface. At the same time, due to the increasing reaction mass associated with a scale-up, the consequences of a thermal runaway are also much higher both in regard to the energy potential of the reaction as well as the amount of potentially harmful substances that could be released in case of an incident. In this context, it is even more important to ensure that such a runaway is prevented by the chosen process conditions.

How a scale-up will influence the temperature and the conversion profile (see **Figure** 6) was evaluated using the model described above. Therefore, simulations with five different reactor volumes (0.5 L, 1.0 L, 2.0 L, 5.0 L, and 15.0 L) were carried out. The composition

of the reaction mixture (10 wt% monomer content), the temperature (60 °C), and the other heat parameters (stirrer speed, flow rate, and temperature in the jacket) were kept constant. The size of the spiral stirrer was scaled-up based on the diameter of the respective reactor.

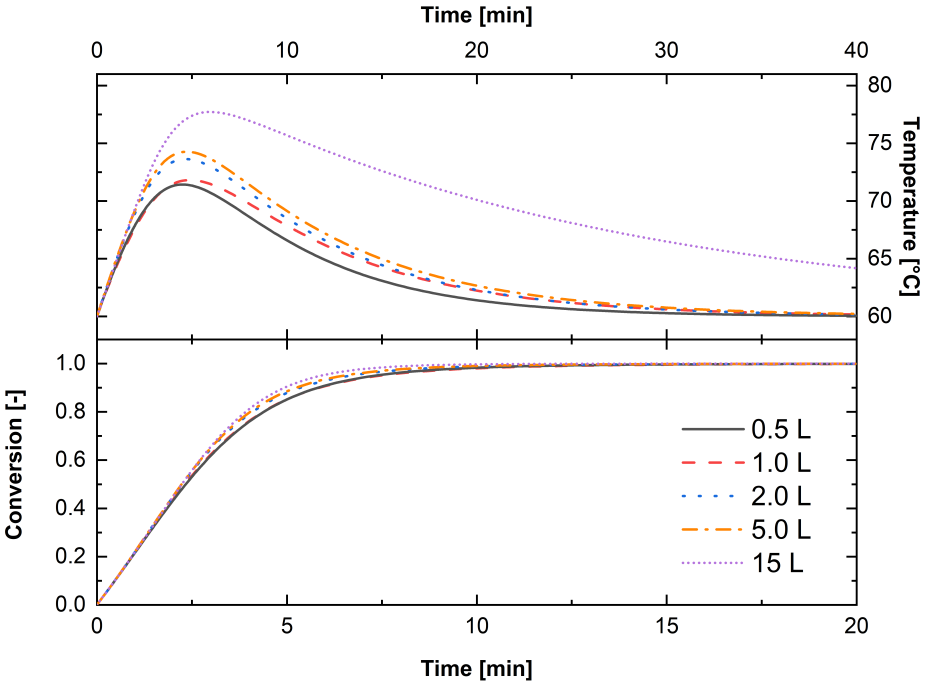

Figure 6: Temperature and conversion profiles of five simulations in different reactor volumes.

As expected, going to larger volumes increases the maximum temperature that is reached over the course of the reaction. The reactors with 0.5 L and 1.0 L as well as 2.0 L and 5.0 L have similar geometric proportions (same diameter with different height) which explains why the associated profiles resemble each other. The maximum temperature is reached later (after 6 min compared to 5 min) in the course of the reaction and the cooling behavior is slower. The reaction in the 15 L reactor differs significantly from the others in its course. The reason for this lies in the different geometric shape of this reactor. It has a larger diameter resulting in a lower surface-to-volume ratio. Compared to the temperature profile, the influence of the reactor size on the conversion behavior is weaker. Because of the risks coming with the scale-up, it is important to evaluate these data with regard to their thermal stability.

This was done in the same way as for the first data set using the criteria of Van Welsenaere (**Table** 4) and Froment and Balakotaiah et. al. (**Figure** 7).

Table 4: Evaluation of the runaway risk of five reactions carried out in reactors with different volumes. A comparison of the maximum temperature difference between reactor and jacket temperature ($\Delta T_{R-J,max}$) as well as the term ($\frac{R \cdot T_R^2}{E_a}$)is given. Whether or not this criterion is met by the reaction is indicated by a ✓ and ×.

Reactor Volume [L]	$\Delta T_{R-J,max}$ [K]	$\frac{R \cdot T_R^2}{E_a}$ [K]	Was criterion meet?
0.5	11.8	14.8	✓
1.0	11.4	14.7	✓
2.0	13.6	14.9	✓
5.0	14.3	15.0	✓
15.0	17.7	15.3	×

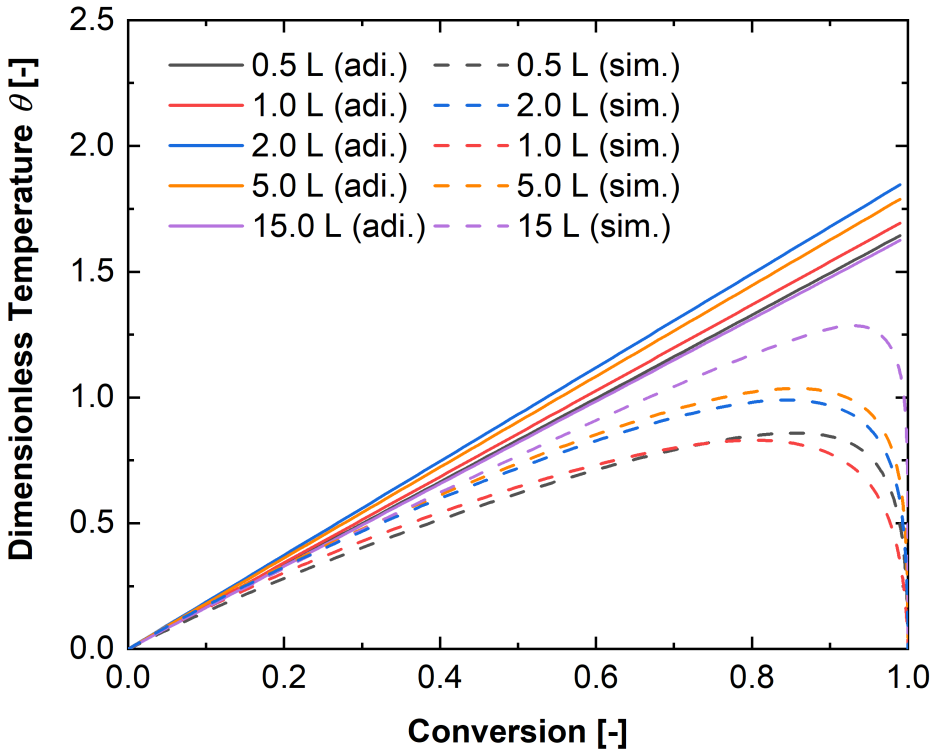

Figure 7: Dimensionless temperature trajectories plotted against the conversion for five reactions carried out at 60 °C, with a monomer content of 10 wt%, and in reactors with five different volumes (increasing from 0.5 L to 15 L). The straight lines represent the theoretical adiabatic case and the dashed lines are the simulated trajectories.

The reaction carried out on a 15 L scale does not meet the criterion of Van Welsenare, while the reaction in the 5 L reactor (14.3 K) is also only slightly below the threshold (15.0 K). Both reactions differ clearly from the adiabatic trajectory in the temperature-conversion plane, while also maintain positive values in the second derivative over the entire reaction course. As already pointed out, the approach in this study does not cover all side reactions and other factors like mixing that could influence the thermal behavior of the reactor. Therefore, the two reactions in the 5 and 15 L reactor should be further optimized in regard to safe process control. As shown in the previous chapters, ways to achieve this include adjusting the coolant temperature, reducing the monomer content, and lowering the starting temperatures. The process parameters in the model were adjusted based on the findings in the previous chapter. The reaction in the 15 L reactor serves as an example. According to the simulations, the increase of temperature could be reduced to 8.8 °C (compared to 17.7 °C with the standard settings) by using a Paravisc stirrer with a stirring speed of 250 min^{-1}, a jacket volume flow rate of 20 L min^{-1}, and a jacket temperature of 40 °C. Using the same settings with a jacket temperature of 50 °C for the 5 L reaction the increase of temperature could be reduced to 5.6 °C compared to 14.3 °C. The data of these simulations are shown in **Figure** S3 in the supporting information.

An alternative to these changes is a transfer of the reaction to a semi-batch process, resulting in a lower heat production rate due to the lower monomer concentration. Another option is the careful selection of the process parameters to keep the reaction controllable despite it being carried out under runaway conditions.[66]

Copolymerization

Anionic polymerization is typically used to synthesize polymers with controlled molecular weight properties. Apart from the synthesis of homopolymers, very often statistical, or block copolymers deriving from the pairs of monomers styrene-isoprene or styrene-vinyl pyridine are synthesized.[68,69] Therefore, it is important that a process model is capable to describe the copolymerizations in order to be useful in a broader field of applications. To meet these requirements, the model presented in this study was extended to a copolymerization model of styrene and isoprene. The extended model was tested based on two different procedures. The monomers were added either together (statistical copolymerization) or subsequently (block copolymers) into the reactor. Both are carried out in the 1 L reactor with a starting temperature of 60 °C and 10 wt% monomer content. Both monomers were added in a weight ratio of 50:50, resulting in a styrene concentration of 39.5 % and isoprene concentration of 60.5 % in regard to the total monomer concentration of 0.81 mol L^{-1}. The other heat transfer parameters are kept at their standard values. The conversion, temperature, and pressure profiles are shown in **Figure** 8.

The model is successfully extended to describe copolymerization and does work both for a statistical as well as a block copolymerization. In the case of statistical copolymerization, the isoprene is the first to react due to the comparatively very low rate coefficient of the cross-reaction between an isoprene anion and styrene.[48] This also leads to a short drop in the reaction rate after the isoprene is fully consumed, which can be observed in the temperature profile. The temperature rises again when the styrene begins to react. The comparison of the two reactions shows that the heat generation of the isoprene polymerization is a bit higher compared to styrene. The reason for this lies in the higher heat of polymerization of isoprene, which is about 1.6 times higher per unit mass compared to styrene. In addition, the rate coefficient of isoprene is slightly higher than that of styrene, resulting also in a higher heat generation rate. In the case of block copolymerization, the two reactions are separated from one another. Isoprene is added after the reaction has cooled down to the

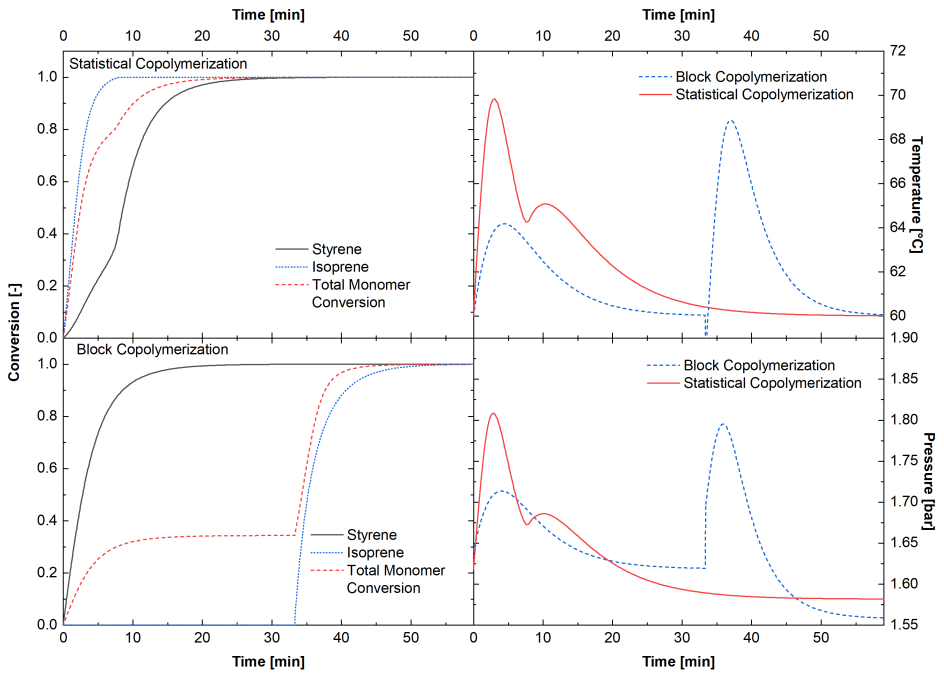

Figure 8: Conversion, temperature, and pressure profiles of a statistical and block copolymerization of styrene and isoprene.

starting temperature. The same is true for the pressure. At this point, the polymerization could be optimize by reducing the time window between the isoprene is added and the time styrene had been fully converted. In order to optimize the reaction, two adjusted recipes were tested. In the optimized recipes, the beginning of the isoprene feed was changed from 33 min to 20 min and 15 min. At these points, the styrene has a conversion of 97 % and 90 %, respectively. The model can now be used to investigate, whether these changes influence the temperature profile, conversion profile, $\overline{M}_n$ profile, or the molecular mass distribution (**Figure** 9).

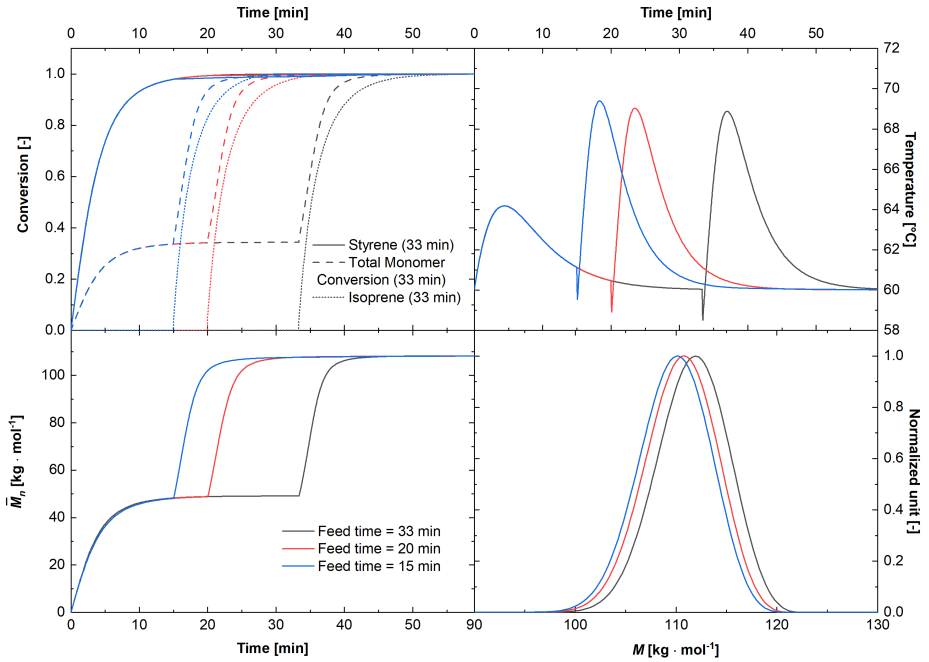

Figure 9: Conversion, temperature, $\overline{M}_n$ profile and molecular mass distribution at the end of the block copolymerization of styrene and isoprene with varying feeding time of the second monomer. The second monomer fed after 33 min, 20 min or 15 min.

A variation of the feeding time leads to a minimal increase of the maximal temperature (from 68 °C to 70 °C) that is reached during the polymerization. At the same time, only a small influence on the molar mass distribution and the $\overline{M}_n$ can be observed. With an earlier start of the isoprene feed, the molar mass distribution is slightly shifted to lower mass (112 kg mol^{-1} to 110 kg mol^{-1}). However, these small changes will not have a significant effect on the polymer properties. On the other hand, the time until full conversion is reached and the time the reactor is cooled down to the starting temperature is reduced by approximately 20 min, resulting in a 33 % reduction of the reaction time.

The simulation with the copolymerization model indicates that a transfer to another monomer system or an extension of the kinetic model can be realized and works in combination with the heat transfer model. If the rate coefficients and physical properties of the involved substances are available, the combined model enables a fast screening of anionic batch polymerization with regard to safety-relevant variables such as the temperature and pressure behavior, as well as other parameters such as conversion, or molecular weight properties. The simulations can be used to optimize the polymerization process to shorter reaction times.

Conclusions

The program Predici was successfully used to model the mass and heat balances of the anionic homopolymerization process of styrene as well as the copolymerization of styrene and isoprene carried out in cyclohexane. The automated computation of the heat transfer properties makes it possible to quickly check the effect of process parameters such as the starting temperature, changes in the formulation of the reaction mixture, heating/cooling temperature, and changes in the reactor size and geometry on the thermal behavior of the reaction system. It can also be used to optimize these parameters. The acquired data can be further used to evaluate safety-relevant questions such as the risk of a thermal runaway.

The basic model can easily be extended in order to describe other monomer systems or copolymerizations. The model has to be validated in the future based on experimental data gathered with inline, online, and offline analytical methods as infrared or Raman spectroscopy (for the conversion), gel permeation chromatography (for the molecular weight properties), and especially calorimetric methods (for the temperature profiles and heat flows). After this is accomplished, the kinetic and heat transfer model can be combined or transferred to a higher dimension in order to include the effects of mass- and heat-transport phenomena by using computational fluid dynamic simulations.

Acknowledgement

This research received no external funding. The authors thank Michael Wulkow, the developer of Predici, for his very helpful, fast and direct support regarding questions about the program. We want also thank Prof. Dr. K. D. Hugenberg and J. Schymura for their help in the acquisition of literature data improving the quality of this work. Help in language-editing from D. Lawrence and J. Schymura is greatfully acknowledged.

Supporting Information

This information is available free of charge via the Internet at http://pubs.acs.org.

Applied Nusselt-correlations, reactor and stirrer geometries, copolymerization model, physical properties of the substances, viscosity profiles, heat capacity of the reactors, pressure calculations, heat introduced by the stirrer, further simulations results of the scale-up

Keywords

anionic polymerization, polymerization modeling, thermal runaway, Predici, copolymers

References

(1) Zhang, L.; Babi, D. K.; Gani, R. New Vistas in Chemical Product and Process Design. *Annual Review of Chemical and Biomolecular Engineering* **2016**, *7*, 557–582.

(2) Ziyatdinov, N. N. Modeling and Optimization of Chemical Engineering Processes and Systems. *Theoretical Foundations of Chemical Engineering* **2017**, *51*, 889–892.

(3) De Oliveira, L. P.; Hudebine, D.; Guillaume, D.; Verstraete, J. J. A Review of Kinetic Modeling Methodologies for Complex Processes. *Oil and Gas Science and Technology* **2016**, *71*, 45.

(4) Cui, J.; Ni, L.; Jiang, J.; Pan, Y.; Wu, H.; Chen, Q. Computational Fluid Dynamics Simulation of Thermal Runaway Reaction of Styrene Polymerization. *Organic Process Research and Development* **2019**, *23*, 389–396.

(5) Roy, S. Calculation of heat of polymerisation: group-contribution method. *Polymer Bulletin* **1999**, *42*, 229–236.

(6) Derboven, P.; Van Steenberge, P. H. M.; Vandenbergh, J.; Reyniers, M.-F.; Junkers, T.; D'hooge, D. R.; Marin, G. B. Improved Livingness and Control over Branching in RAFT Polymerization of Acrylates: Could Microflow Synthesis Make the Difference? *Macromolecular Rapid Communications* **2015**, *36*, 2149–2155.

(7) Zhao, L.; Zhu, W.; Papadaki, M. I.; Mannan, M. S.; Akbulut, M. Probing into Styrene Polymerization Runaway Hazards: Effects of the Monomer Mass Fraction. *ACS Omega* **2019**, *4*, 8136–8145.

(8) Yang, L.; Nieves-Remacha, M. J.; Jensen, K. F. Simulations and analysis of multiphase transport and reaction in segmented flow microreactors. *Chemical Engineering Science* **2017**, *169*, 106–116.

(9) Nieves-Remacha, M. J.; Kulkarni, A. A.; Jensen, K. F. OpenFOAM Computational Fluid Dynamic Simulations of Single-Phase Flows in an Advanced-Flow Reactor. *Industrial and Engineering Chemistry Research* **2015**, *54*, 7543–7553.

(10) Serra, C.; Schlatter, G.; Sary, N.; Schönfeld, F.; Hadziioannou, G. Free radical polymerization in multilaminated microreactors: 2D and 3D multiphysics CFD modeling. *Microfluidics and Nanofluidics* **2007**, *3*, 451–461.

(11) Milewska, A.; Rudniak, L.; Molga, E. CFD modelling and divergence criterion for safety of chemical reactors. *Computer Aided Chemical Engineering* **2005**, *20*, 259–264.

(12) Milewska, A.; Molga, E. J. CFD simulation of accidents in industrial batch stirred tank reactors. *Chemical Engineering Science* **2007**, *62*, 4920–4925.

(13) Wulkow, M. The simulation of molecular weight distributions in polyreaction kinetics by discrete Galerkin methods. *Macromolecular Theory and Simulations* **1996**, *5*, 393–416.

(14) Deuflhard, P.; Wulkow, M. Computational treatment of polyreaction kinetics by orthogonal polynomials of a discrete variable. *IMPACT of Computing in Science and Engineering* **1989**, *1*, 269–301.

(15) Schütte, C.; Wulkow, M. A Hybrid galerkin-monte-carlo approach to higher-dimensional population balances in polymerization kinetics. *Macromolecular Reaction Engineering* **2010**, *4*, 562–577.

(16) Wulkow, M. Computer aided modeling of polymer reaction engineering-The status of predici, 1 - simulation. *Macromolecular Reaction Engineering* **2008**, *2*, 461–494.

(17) Zetterlund, P. B.; Yamazoe, H.; Yamada, B. Free radical bulk polymerization of styrene: Simulation of molecular weight distributions to high conversion using experimentally obtained rate coefficients. *Macromolecular Theory and Simulations* **2003**, *12*, 379–385.

(18) Eckes, D.; Busch, M. Coupled Deterministic and Stochastic Modeling of an Industrial Multi-Zone LDPE Autoclave Reactor. *Macromolecular Symposia* **2016**, *360*, 23–31.

(19) Ren, S.; Vivaldo-Lima, E.; Dubé, M. A. Modeling of the copolymerization kinetics of n-butyl acrylate and D-limonene using PREDICI. *Processes* **2016**, *4*, 1.

(20) Gómez-Reguera, J. A.; Vivaldo-Lima, E.; Gabriel, V. A.; Dubé, M. A. Modeling of the free radical copolymerization kinetics of n-butyl acrylate, methyl methacrylate and 2-ethylhexyl acrylate using PREDICI. *Processes* **2019**, *7*, 395.

(21) Nikitin, A. N.; Hutchinson, R. A.; Wang, W.; Kalfas, G. A.; Richards, J. R.; Bruni, C. Effect of Intramolecular Transfer to Polymer on Stationary Free-Radical Polymerization of Alkyl Acrylates, 5 - Consideration of Solution Polymerization up to High Temperatures. *Macromolecular Reaction Engineering* **2010**, *4*, 691–706.

(22) De Keer, L.; Van Steenberge, P. H. M.; Reyniers, M.; Marin, G. B.; Hungenberg, K.; Seda, L.; D'hooge, D. R. A complete understanding of the reaction kinetics for the industrial production process of expandable polystyrene. *AIChE Journal* **2017**, *63*, 2043–2059.

(23) Aldana-García, M. A.; Palacios, J.; Vivaldo-Lima, E. Modeling of the microwave initiated emulsion polymerization of styrene. *Journal of Macromolecular Science - Pure and Applied Chemistry* **2005**, *42 A*, 1207–1225.

(24) Reynhout, X. E. E.; Meuldijk, J.; Drinkenburg, B. A. H.; Iedema, P. D.; Wulkow, M. A novel method to model emulsion polymerization kinetics: The explicit radical-particle size distribution approach. *Polymer - Plastics Technology and Engineering* **2005**, *44*, 707–740.

(25) Barner-Kowollik, C.; Quinn, J. F.; Morsley, D. R.; Davis, T. P. Modeling the reversible addition-fragmentation chain transfer process in cumyl dithiobenzoate-mediated styrene homopolymerizations: Assessing rate coefficients for the addition-fragmentation equilibrium. *Journal of Polymer Science, Part A: Polymer Chemistry* **2001**, *39*, 1353–1365.

(26) Wulkow, M.; Busch, M.; Davis, T. P.; Barner-Kowollik, C. Implementing the Reversible Addition-Fragmentation Chain Transfer Process in PREDICI. *Journal of Polymer Science, Part A: Polymer Chemistry* **2004**, *42*, 1441–1448.

(27) Kandelhard, F.; Schuldt, K.; Schymura, J.; Georgopanos, P.; Abetz, V. Model-Assisted

Optimization of RAFT Polymerization in Micro-Scale Reactors — A Fast Screening Approach. *Macromolecular Reaction Engineering* **2021**, *2000058*, 1–17.

(28) Whitfield, R.; Parkatzidis, K.; Truong, N. P.; Junkers, T.; Anastasaki, A. Tailoring Polymer Dispersity by RAFT Polymerization: A Versatile Approach. *Chem* **2020**, *6*, 1340–1352.

(29) Paulus, F.; Weiss, M. E. R.; Steinhilber, D.; Nikitin, A. N.; Schütte, C.; Haag, R. Anionic ring-opening polymerization simulations for hyperbranched polyglycerols with defined molecular weights. *Macromolecules* **2013**, *46*, 8458–8466.

(30) Ahmadnian, F.; Reichert, K. H. Kinetic studies of polyethylene terephthalate synthesis with titanium-based catalyst. *Macromolecular Symposia* **2007**, *259*, 188–196.

(31) Katzer, J. Hydrolytic caprolactam polymerization - Progress in dynamic simulation. *Macromolecular Reaction Engineering* **2014**, *8*, 658–665.

(32) Kim, D. M.; Nauman, E. B. Nonterminating Polymerizations in Continuous Flow Systems. *Industrial and Engineering Chemistry Research* **1997**, *36*, 1088–1094.

(33) Kim, D. M.; Nauman, E. B. Anionic polymerization of styrene in a tubular reactor. *Industrial and Engineering Chemistry Research* **1999**, *38*, 1856–1862.

(34) Xie, L.; Zhu, L. T.; Luo, Z. H. Computational Fluid Dynamics Simulation of Multiscale Mixing in Anionic Polymerization Tubular Reactors. *Chemical Engineering and Technology* **2016**, *39*, 857–864.

(35) Domanskyi, S.; Gentekos, D. T.; Privman, V.; Fors, B. P. Predictive design of polymer molecular weight distributions in anionic polymerization. *Polymer Chemistry.* **2020**, *11*, 326–336.

(36) Meszéna, Z. G.; Johnson, A. F. Prediction of the spatial distribution of the average

molecular weights in living polymerisation reactors using CFD methods. *Macromolecular Theory and Simulations* **2001**, *10*, 123–135.

(37) Saban, M.; Liebermann, G.; Jay, A.; Shi, A.-C.; Ro, N.; Dale, W.; Forgione, P. Piloting of anionic polymerization of styrene in tetrahydrofurant. *The Canadian Journal of Chemical Engineering* **2000**, *78*, 320–329.

(38) Rivero, P.; Herrera, R. Modeling the kinetics of anionic polymerization in cyclohexane as a non-complexing solvent. *Journal of Polymer Research* **2011**, *18*, 519–526.

(39) Rodriguez-Guadarrama, L. Modeling of Anionic Polymerization of Isoprene in an Industrial Reactor. *Macromolecular Reaction Engineering* **2019**, *13*, 1–7.

(40) Kandelhard, F. Die Reaktionskalorimetrie zur Prozesskontrolle bei unterschiedlicher Prozessführung. Ph.D. thesis, Universität Hamburg, 2019.

(41) *VDI-wärmeatlas*; Springer Berlin Heidelberg, 2006; p 1136–1162.

(42) Malotherm XC Data Sheet. `http://www.sasolgermany.de/fileadmin/images/marlotherm/MARLOTHERM_XC_info_e_.pdf`, Date accessed: 24.02.2021.

(43) Mohan, P.; Nicholas Emery, A.; Al-Hassan, T. Review heat transfer to Newtonian fluids in mechanically agitated vessels. *Experimental Thermal and Fluid Science* **1992**, *5*, 861–883.

(44) Kleiber, M.; Joh, R. *VDI-wärmeatlas*; Springer Berlin Heidelberg, 2013; pp 1136–1162.

(45) Hsieh, H. L. Kinetics of polymerization of butadiene, isoprene, and styrene with alkyllithiums. Part II. Rate of initiation. *Journal of Polymer Science Part A: General Papers* **1965**, *3*, 163–172.

(46) Hungenberg, K. D.; Wulkow, M. *Modeling and Simulation in Polymer Reaction Engineering: A Modular Approach*, 1st ed.; Wiley-VCH, 2018.

(47) Hugenberg, K. D.; Bandermann, F.; Janko, L. Anionic polymerization of styrene at high temperatures. *DECHEMA Monographs* **1995**, *131*, 387–399.

(48) Steube, M.; Johann, T.; Plank, M.; Tjaberings, S.; Gröschel, A. H.; Gallei, M.; Frey, H.; Müller, A. H. E. Kinetics of Anionic Living Copolymerization of Isoprene and Styrene Using in Situ NIR Spectroscopy: Temperature Effects on Monomer Sequence and Morphology. *Macromolecules* **2019**, *52*, 9299–9310.

(49) Styrene Product Data Sheet. `https://cameochemicals.noaa.gov/chris/STY.pdf`, Date accessed: 24.02.2021.

(50) Cyclohexane Product Data Sheet. `https://cameochemicals.noaa.gov/chris/CHX.pdf`, Date accessed: 24.02.2021.

(51) Gaur, U.; Wunderlich, B. B.; Wunderlich, B. Heat Capacity and Other Thermodynamic Properties of Linear Macromolecules. VII. Other Carbon Backbone Polymers. *Journal of Physical and Chemical Reference Data* **1983**, *12*, 29–63.

(52) Brandrup, J.; Immergut, E.; Grulke, E. *Polymer Handbook*; A Wiley-Interscience Publication; Wiley, 1999.

(53) Cortese, B.; Noel, T.; de Croon, M. H.; Schulze, S.; Klemm, E.; Hessel, V. Modeling of Anionic Polymerization in Flow With Coupled Variations of Concentration, Viscosity, and Diffusivity. *Macromolecular Reaction Engineering* **2012**, *6*, 507–515.

(54) Xie, L.; Zhu, L.-T.; Luo, Z.-H. Computational Fluid Dynamics Simulation of Multiscale Mixing in Anionic Polymerization Tubular Reactors. *Chemical Engineering & Technology* **2016**, *39*, 857–864.

(55) Bywater, S.; Worsfold, D. J. Alkyllithium anionic polymerization initiators in hydrocarbon solvents. *Journal of Organometallic Chemistry* **1967**, *10*, 1–6.

(56) Johnson, A. F.; Worsfold, D. J. Anionic polymerization of butadiene and styrene. *Journal of Polymer Science Part A: General Papers* **1965**, *3*, 449–455.

(57) Isoprene Product Data Sheet. `https://cameochemicals.noaa.gov/chris/IPR.pdf`, Date accessed: 19.03.2021.

(58) Dreyer, R.; Martin, W.; Weber, U. v. Die Sättigungsdampfdrucke von Benzol, Toluol, Äthylbenzol, Styrol, Cumol and Brombenzol zwischen 10 und 760 Torr. *Journal für Praktische Chemie* **1955**, *1*, 324–328.

(59) Gubkov, A. N.; Fermor, N. A.; Smirnov, N. I. Vapor pressure of mono-poly systems. 1964; `https://webbook.nist.gov/cgi/cbook.cgi?ID=C78795&#38;Mask=4`, Date accessed: 24.02.2021.

(60) Kerns, W. J.; Anthony, R. G.; Eubank, P. T. Volumetric Properties of Cyclohexane Vapor. 1974; `https://webbook.nist.gov/cgi/cbook.cgi?ID=C110827&#38;Mask=4#ref-23`, Date accessed: 24.02.2021.

(61) Westerterp, K. R.; Molga, E. J. Safety and runaway prevention in batch and semibatch reactors - A review. *Chemical Engineering Research and Design* **2006**, *84*, 543–552.

(62) Welsenaere, R. J. v.; Froment, G. F. Parametric sensitivity and runaway in fixed bed catalytic reactors. *Chemical Engineering Science* **1970**, *25*, 1503–1516.

(63) Balakotaiah, V.; Kodra, D.; Nguyen, D. Runaway limits for homogeneous and catalytic reactors. *Chemical Engineering Science* **1995**, *50*, 1149–1171.

(64) Adler, J.; Enig, J. W. The critical conditions in thermal explosion theory with reactant consumption. *Combustion and Flame* **1964**, *8*, 97–103.

(65) Khuong, K. S.; Jones, W. H.; Pryor, W. A.; Houk, K. N. The mechanism of the self-initiated thermal polymerization of styrene. Theoretical solution of a classic problem. *Journal of the American Chemical Society* **2005**, *127*, 1265–1277.

(66) Rodriguez-Guadarrama, L. Thermal runaway risk analysis in styrenic block copolymer production. *Process Safety Progress* **2020**, e12227.

(67) Johnson, M.; Heggs, P. J.; Mahmud, T. Assessment of Overall Heat Transfer Coefficient Models to Predict the Performance of Laboratory-Scale Jacketed Batch Reactors. *Organic Process Research and Development* **2016**, *20*, 204–214.

(68) Georgopanos, P.; Filiz, V.; Handge, U. A.; Abetz, V. Chemical modification, thermal characterization and dielectric spectroscopy of polystyrene-block-polyisoprene diblock copolymers. *Macromolecular Chemistry and Physics* **2016**, *211*, 1293–1304.

(69) Kollmetz, T.; Georgopanos, P.; Handge, U. A. Rheology in shear and elongation and dielectric spectroscopy of polystyrene-block-poly (4-vinylpyridine) diblock copolymers. *Polymer* **2017**, *129*, 68–82.